Cell Metabolism, Volume *17*

Supplemental Information

MICU1 Controls Both the Threshold and Cooperative Activation of the Mitochondrial Ca^{2+} Uniporter

György Csordás, Tünde Golenár, Erin L. Seifert, Kimberli J. Kamer, Yasemin Sancak, Fabiana Perocchi, Cynthia Moffat, David Weaver, Sergio de la Fuente Perez, Roman Bogorad, Victor Koteliansky, Jeffrey Adijanto, Vamsi K. Mootha, and György Hajnóczky

Inventory of Supplemental Information

Supplemental figures and legends

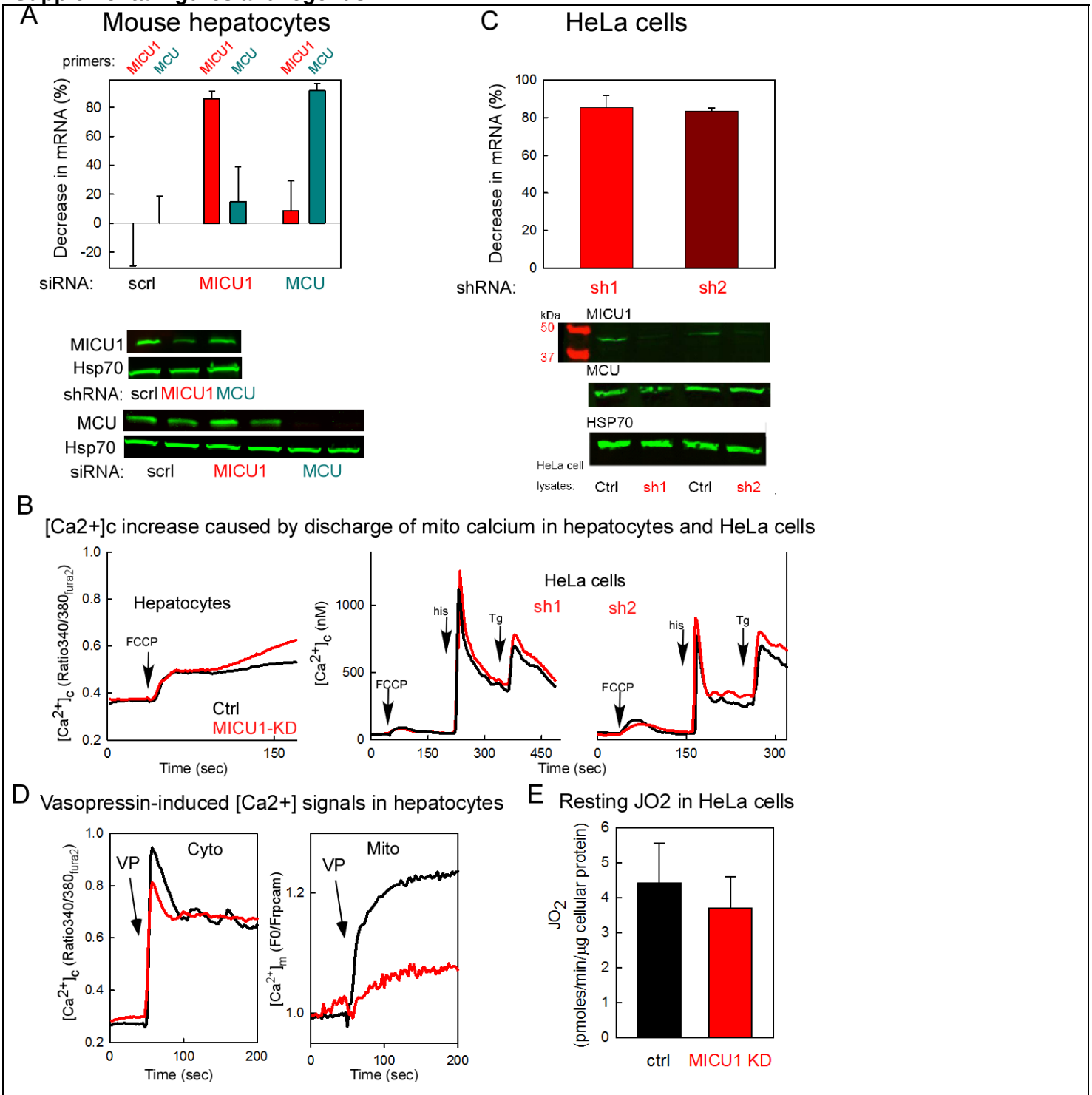

Figure S1, related to Fig1. Basal and agonist-induced increases in $[Ca^{2+}]_m$ and cellular O_2 consumption (JO_2) in MICU1-KD cells

(**A**) MICU1 and MCU mRNA and protein levels in hepatocytes upon in vivo silencing of MICU1 and MCU, respectively (mRNA: mean±SE of 3-5 biological replicates; protein: MICU1: 1, MCU: 2 representative biological replicates). **(B)** $[Ca^{2+}]_c$ increase-induced by a mitochondrial uncoupler, FCCP in non-stimulated Ctrl and MICU1-KD primary hepatocytes (left) and stable HeLa cells (sh1 middle, sh2 right). Mean traces of 42 Ctrl and 40 MICU1-KD hepatocytes; and 70 Ctrl and 75 sh1; and 52 Ctrl and 40 sh2 HeLa cells. **(C)** MICU1 mRNA is decreased by ~80% in sh1 and sh2 clones. RNA was isolated (see Supplemental Methods) from sh1 and sh2 cultures and corresponding LacZ controls (n=3-4 for all). Protein levels of MICU1 are decreased, whereas MCU and Hsp70 (loading control) are unaltered in lysates of sh1 and sh2 HeLa cells. **(D)** Vasopressin (VP, 100nM)-induced $[Ca^{2+}]_c$ and $[Ca^{2+}]_m$ rise in hepatocytes (mean traces of n=11 for ctrl, n=30 for MICU1-KD). **(E)** Resting JO_2 in Ctrl and MICU1-KD stable HeLa cells (n=4).

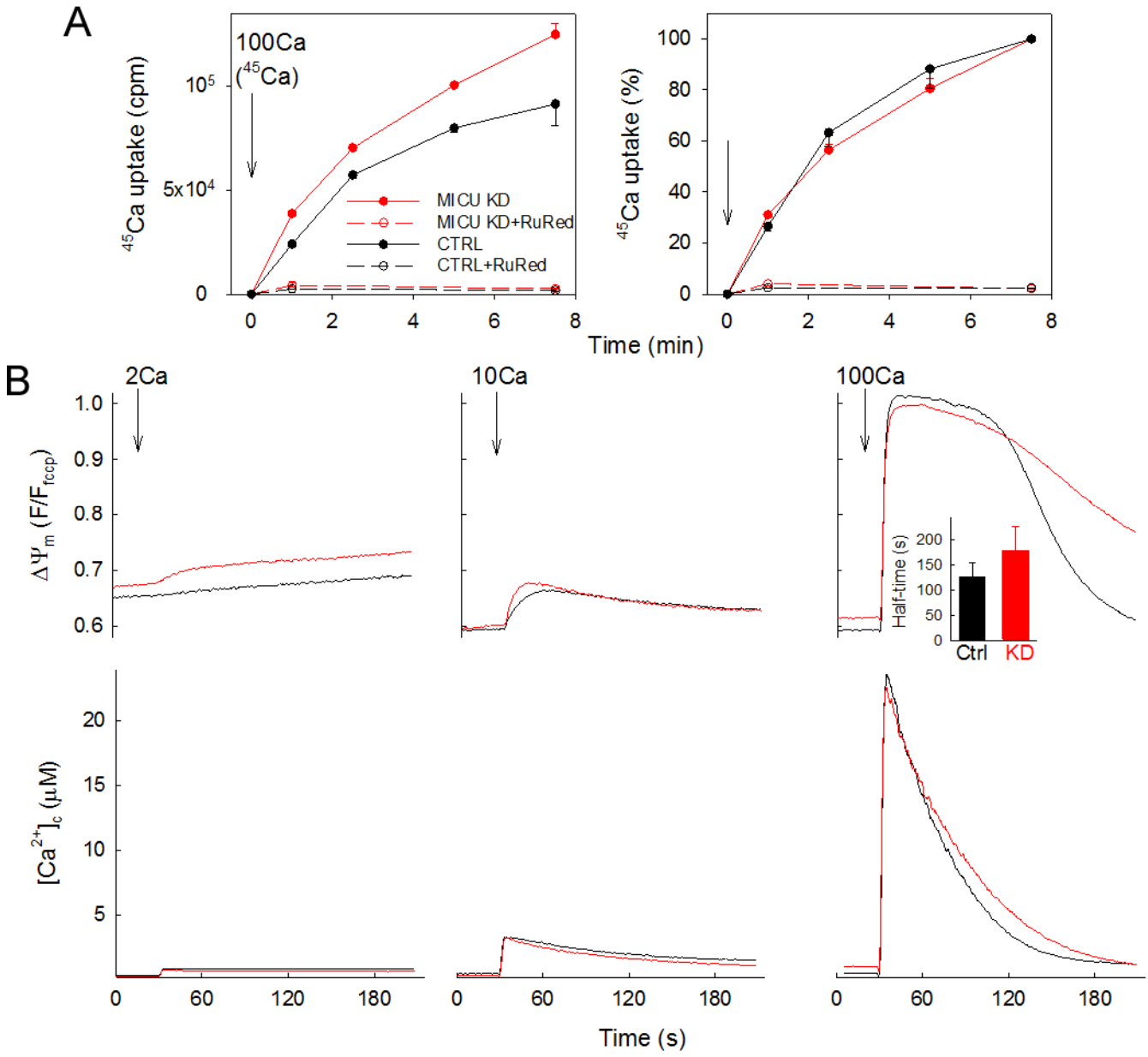

Figure S2, related to Fig2. Mitochondria are sensitized to Ca^{2+} uptake-induced depolarization in MICU1-KD permeabilized cells

(**A**) Uptake of $^{45}Ca^{2+}$ in suspensions of permeabilized cells incubated in the presence of Tg (2 μM). When $^{45}Ca^{2+}$ was added the $[Ca^{2+}]_c$ was increased from <20nM to approx. 30 μM (0s). Left: The time course of $^{45}Ca^{2+}$ accumulation is shown both in the absence and presence of RuRed (3 μM) (n=3). Right: Time course normalized to 450s uptake (n=6).

(**B**) In suspensions of permeabilized stable MICU1-KD (sh1) and Ctrl HeLa cells, $\Delta\Psi_m$ was simultaneously monitored with $[Ca^{2+}]_c$ during addition of 2, 10 and 100μM $CaCl_2$ (left, middle and right, respectively). Time courses show that the augmented $[Ca^{2+}]_c$ clearance by MICU1-KD mitochondria was associated with an enhanced depolarization during $[Ca^{2+}]_c$ increases to 1-3μM (left, middle). Furthermore, in MICU1-KD a prolonged loss of $\Delta\Psi_m$ occurred during large $[Ca^{2+}]_c$ elevations (>20μM, right, bar charts, n=7, $p<0.05$).

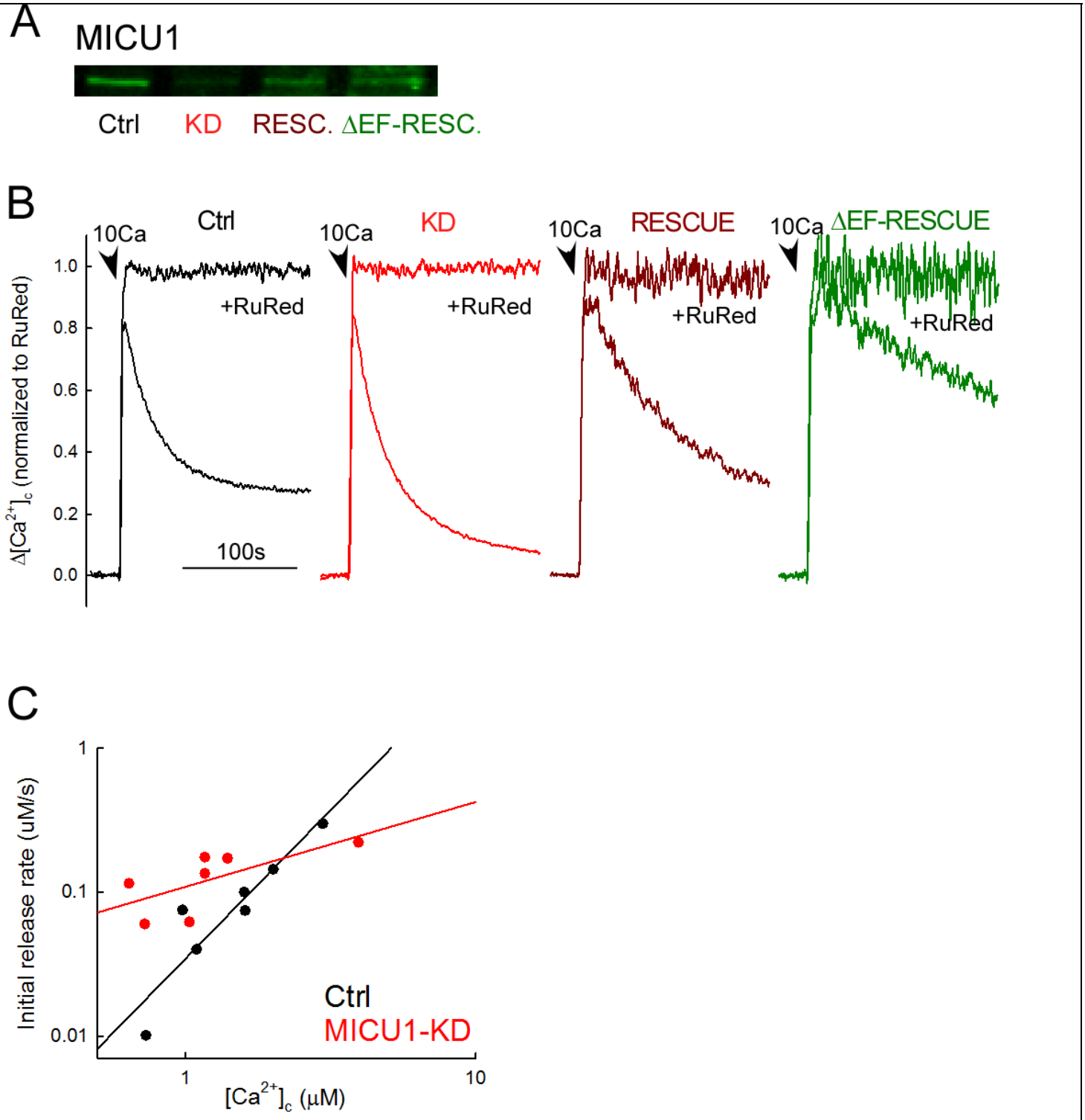

Figure S3, related to Fig3. Maintenance of the $[Ca^{2+}]_c$ threshold of the activation of the uniporter by MICU1 is independent of its EF-hands

(A) Protein levels of MICU1 in HeLa whole cell lysates of Ctrl, MICU1-KD (stable, sh1) and MICU1-KD rescued with either wild type MICU1 (RESC.) or EF-hand mutant MICU1 (ΔEF-RESC.). **(B)** Mitochondrial clearance of a 10 μM $CaCl_2$ pulse in permeabilized Ctrl, MICU1-KD, MICU1-KD rescued with wild type MICU1 (RESCUE), and MICU1-KD rescued with EF-hand mutant MICU1 (ΔEF-RESCUE) cells (from left to right). **(C)** Double-logarithmic plot of the initial rates of FCCP-induced $[Ca^{2+}]_c$ rises as a function of $[Ca^{2+}]_c$ at the time of FCCP addition from several recordings in Ctrl and MICU1-KD HeLa cells with linear regressions. (**D**) Instantaneous rate of FCCP-induced Ca^{2+} efflux at each $[Ca^{2+}]_c$ (0.5μM binning) obtained via differentiation of the initial 30-60s of the $[Ca^{2+}]_c$ rises caused by FCCP. RESCUE vs ΔEF-RESCUE MICU1 (n=4). 0.5 μM [Ca2+]c binning.

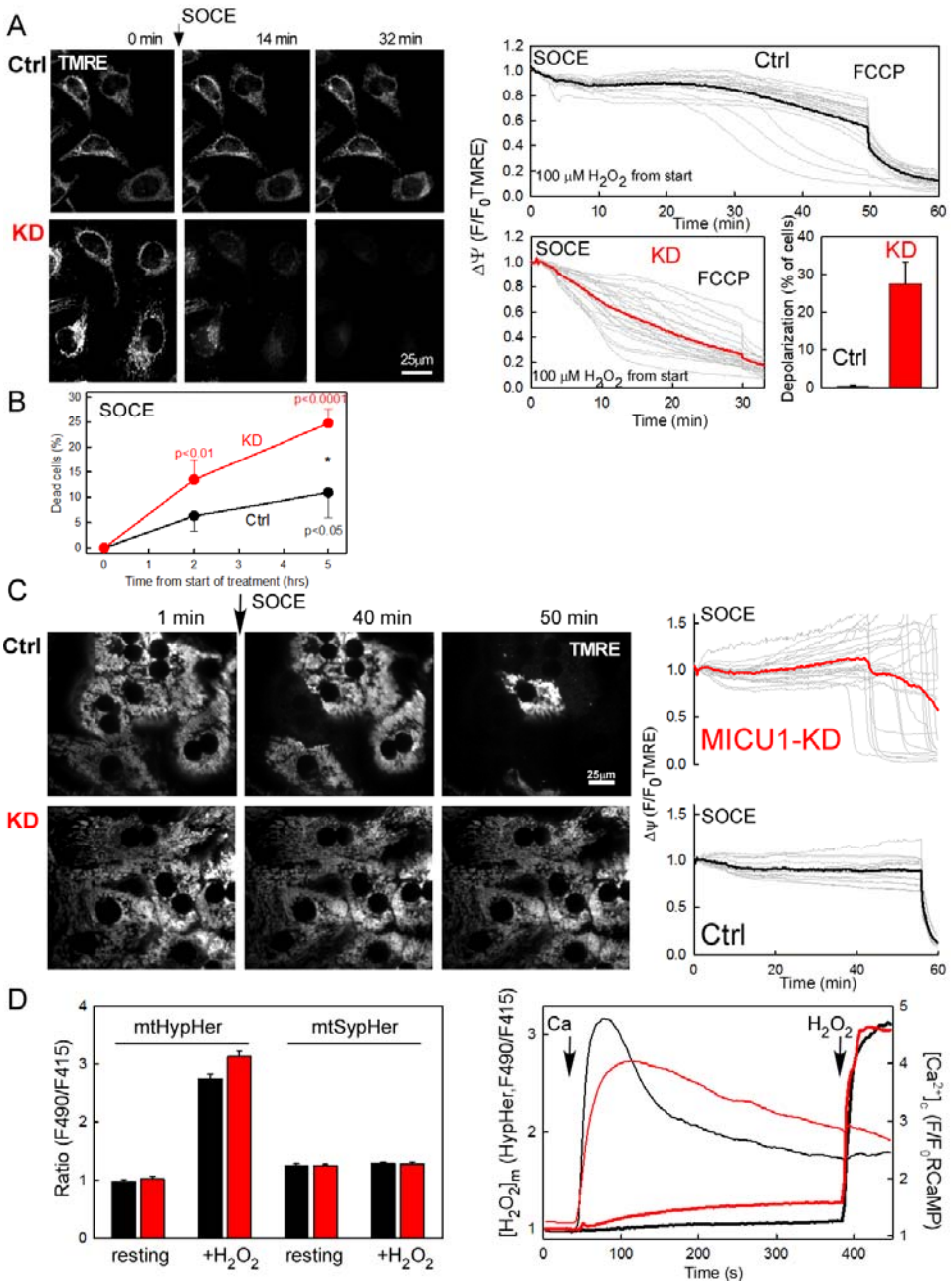

Figure S4, related to Fig5. Increased sensitivity of MICU1-KD cells to delayed mitochondrial Ca^{2+} dysregulation: role of ROS (A) Dissipation of $\Delta\Psi_m$ elicited by Tg-induced mitochondrial Ca^{2+} overloading in 100μM H_2O_2-pre-treated Ctrl and stable MICU1-KD HeLa cells. Left: TMRE fluorescence images recorded during prolonged Ca^{2+} entry. Right: Time courses of TMRE fluorescence in individual cells. Lower right: The lag time calculated for 50% loss of TMRE fluorescence (n=23 and 21 for Ctrl and MICU1-KD, respectively, $p<0.01$). **(B)** Quantification of cell death induced by Tg and H_2O_2 (n = 5). **(C)** Dissipation of $\Delta\Psi_m$ elicited by Tg-induced mitochondrial Ca^{2+} overloading in 100μM H_2O_2-pre-treated Ctrl and MICU1-KD primary hepatocytes. Left: TMRE fluorescence images recorded during prolonged Ca^{2+} entry. Right: Time courses of TMRE fluorescence in individual cells. FCCP was added at 57min. Loss of the $\Delta\Psi_m$ was observed in 0/16 Ctrl cells and 11/22 MICU1-KD cells. **(D)** Measurement of resting and SOCE-stimulated mitochondrial matrix $[H_2O_2]$ ($[H_2O_2]_m$) response with mtHyPer in Ctrl and stable MICU1-KD HeLa cells. To uncover possible pH-dependent changes in the HyPer fluorescence, measurements were also performed with mtSypHer, the H_2O_2 desensitized version of HyPer. Bar charts on the left show the lack of difference in the resting mtHyPer and mtSypHer ratios between Ctrl and MICU1-KD cells. H_2O_2 was added as a reference (mt-HyPer: n=27 for both Ctr and MICU1-KD; mt-SypHer: n=21 and 30 for Ctrl, and MICU1-KD, respectively). Time-course traces (thick lines) on the right show a gradual increase in the mtHyPer ratio only in MICU1-KD ($p<0.05$) during SOCE. The simultaneously recorded $[Ca^{2+}]_c$ is shown with thin lines.

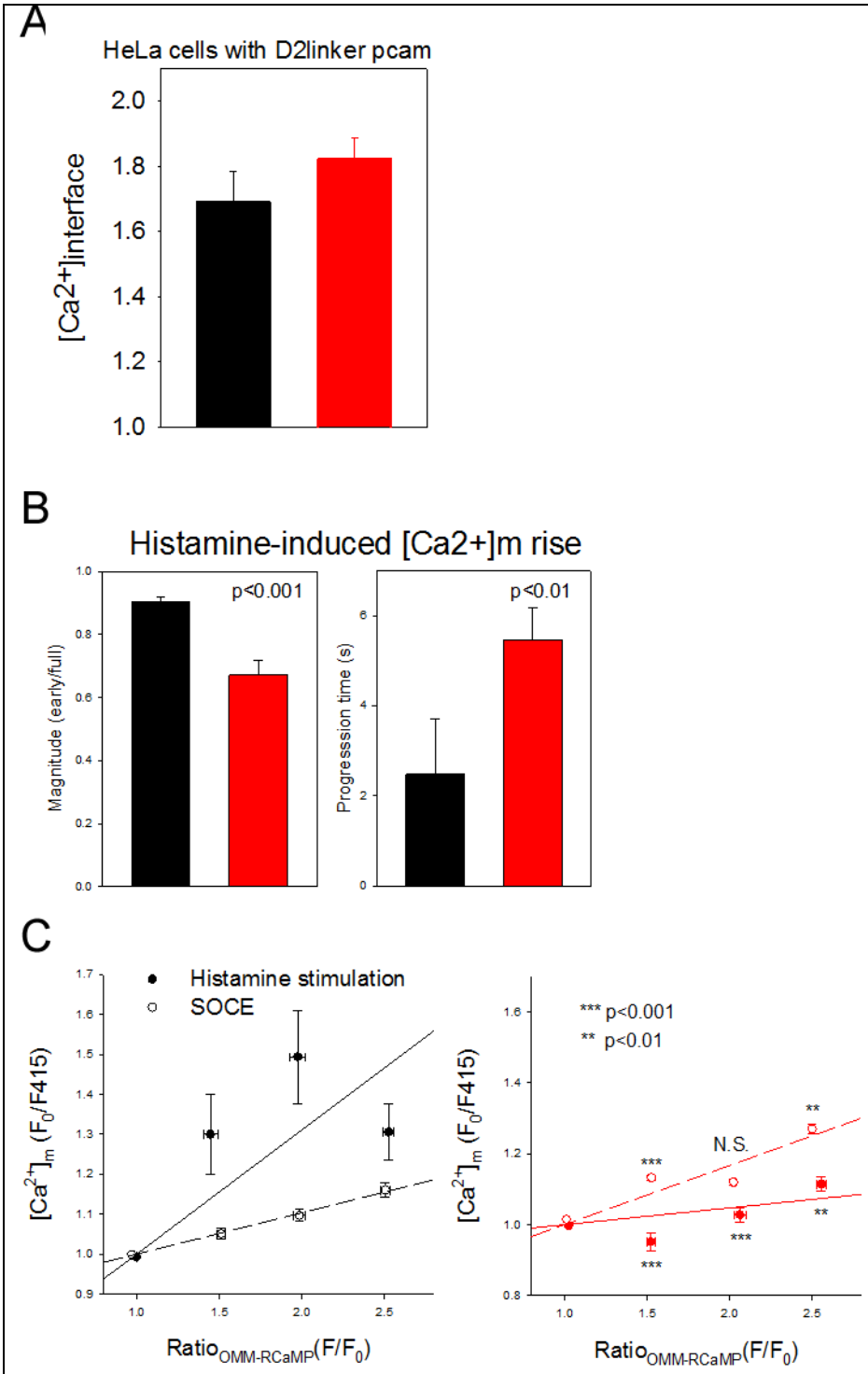

Figure S5, related to Fig6. Ineffective Ca^{2+} delivery to the mitochondria during IP3-linked Ca^{2+} mobilization in MICU1-deficient cells

(A) Similar high [Ca^{2+}] microdomains in Ctrl and stable MICU1-KD HeLa cells at the ER-mitochondrial interface ($[Ca^{2+}]_{interface}$) during histamine (100μM)-induced Ca^{2+} mobilization (n=32 for Ctrl, n=37 for MICU1-KD). The peak D2 linker pericam ratios correspond to approx. 10μM $[Ca^{2+}]_{interface}$ (Csordas et al., 2010; Giacomello et al., 2010). **(B)**. Slow progression of the $[Ca^{2+}]_m$ signal in MICU1-KD cells is reflected in the small response occurring at the time of the $[Ca^{2+}]_c$ peak (early) relative to the maximal response (full)(left) and in the relatively long time elapsed between the $[Ca^{2+}]_c$ and $[Ca^{2+}]_m$ peaks (2nd from left). (**C**) When $[Ca^{2+}]_m$ was recorded simultaneously with and plotted against the local $[Ca^{2+}]_c$ at the mitochondrial surface (measured by RCaMP targeted to the outer mitochondrial membrane), unlike the Ctrl cells (left), the MICU1-KD cells failed to show greater response to histamine (continuous line) than to SOCE (dashed, right).

Supplemental Experimental Procedures:

Chemicals: Standard chemicals were purchased from Fisher Scientific or Sigma-Aldrich. IP_3 and thapsigargin was from LC Laboratories (Woburn, MA) or from Enzo Life Sciences (Plymouth Meeting, PA). Fluorescent Ca^{2+}-indicator dyes, and Pluronic F-127 were from Molecular Probes or Teflabs. Chelex 100 Sodium form was purchased from BioRad.

DNA constructs: Ca^{2+} sensing fluorescent proteins, inverse and ratiometric pericams (Nagai et al., 2001) and a ratiometric pH sensor, SypHer (Poburko et al., 2011) targeted to the mitochondrial matrix were a gift from Drs. Atsushi Miyawaki (RIKEN) and Nicolas Demaurex (University of Geneva), respectively.

Transient expression:. Isolated hepatocytes were infected using adenovirus encoding mitochondria-targeted ratiometric pericam (5 PFU/cell, Vector Biolabs). HeLa cells were transiently transfected with plasmid DNA (4-6ug/ml) using Lipofectamine 2000 (4-10ul/ml, from Invitrogen) for 24-48h.

Cells: Isolated mouse hepatocytes were seeded in William's E medium supplemented with 2mM glutamine, 1μM dexamethasone, 50μg/ml gentamycin, 1% penicillin/streptomycin, and 10% newborn calf serum, then maintained in the same medium without serum. HeLa cells were grown in DMEM, 10% FBS and antibiotics for selection as described earlier (Perocchi et al., 2010).

In vivo silencing of MICU1 or MCU in mouse liver: Each mouse received 0.5 μg/g body weight siRNA formulated into lipidoid nanoparticles against MICU1 or MCU or luciferase (control) via the tail vein, once per week, for 4 weeks (Baughman et al., 2011).

Stable and short-term silencing of MICU1 or MCU in HeLa cells: Stable expression of shRNAs and wild-type and mutant proteins has been described (Baughman et al., 2011; Perocchi et al., 2010). For short-term silencing, HeLa cells were transfected with the siRNA version of the same sh1 and sh2 hairpins used for stable cells (Ambion) or with scrambled siRNA for 48hr using Oligofectamine (Invitrogen).

RNA, cDNA and qPCR protocols: Total RNA of cells was extracted using Trizol® (Invitrogen, Carlsbad, CA) according to manufacturer's specifications. Purified RNA was subsequently treated with RQ1 DNase (Promega, Madison, WI, USA) at 37 ^{o}C for 30 mins. Total RNA concentration was measuring using Qubit® Fluorometer (Invitrogen, Carlsbad, CA). RNA was reverse transcribed using oligo$(dT)_{20}$ primers and SuperScript III (Invitrogen, Carlsbad, CA). qPCR reactions for gene expression studies were performed using ITaq SYBR green Supermix with ROX (BIO-RAD, Hercules, CA) in 20 uL reactions (20 ng cDNA/reactions). qPCR was performed using Eppendorf Mastercycler® ep realplex. Primers were designed using Eurofins Primer Design Tool. Custom oligos were purchased from Eurofins MGW Operon (Huntsville, AL). Primer sequences for human *MICU1* are Forward: 5'-ACAGTGGCTAAAGTGGAGC-3', Reverse: 5'-GTTTGGGTAAAGCGAAGTCC-3'; for mouse *MICU1*are Forward: 5'-AACAGCAAGAAGCCTGACAC-3', Reverse: 5'-CTCATTGGGCGTTATGGAG-3'; for mouse *MCU* are Forward: 5'-TACTCACCAGATGGCGTTC-3', Reverse: GTCCTCTAACCTCTCCACqPCR data were analyzed using the comparative $2^{-\Delta\Delta Ct}$ method (Schmittgen and Livak, 2008). Ct of the gene of interest was referenced to that of β-actin.

Immunoblot analysis: Lysates from membrane fractions and whole cells were made using RIPA buffer. Western blot analysis was performed as described (Roy et al., 2009). Primary antibodies (polyclonal) were anti–MICU1 (Abcam), and anti-MCU (SIGMA). Monoclonal Anti-Hsp70 (Thermo Scientific) was used as the loading control. Samples for the topology analysis experiments were analyzed by western blot using the following antibodies: MICU1 (homemade), HSP60, ATP5a (Abcam), TIMM23 (BD Sciences), OXA1L (BD Sciences), TOMM20 (Santa Cruz), CYCS (MitoSciences), and MCU (Sigma).

MICU1 Topology Analysis: Localization analysis was performed according to (Sato and Mihara, 2010). HEK-293T cell crude mitochondria were isolated by differential centrifugation as described previously (Perocchi et al., 2010). After isolation, the mitochondrial pellet was resuspended in 280mM sucrose with 10mM Hepes (pH 7.2). Mitochondria isolated from HEK-293T cells (10 ug per condition) were treated with different digitonin concentrations (0%-1%) or 1% Triton X-100 along with 100 ug/ml Proteinase K (PK) at room temperature. After 15', 10 mM PMSF was added to stop the digestion and SDS sample buffer was added. Alkaline carbonate extraction was performed according to (Ryan et al., 2001). Briefly, 100 μg of mitochondria were pelleted and resuspended in 200 uL of 100 mM $NaCO_3$ buffer adjusted to either pH 10 or pH 11.5. After

incubation on ice for 30', samples were centrifuged at 100,000 rpm for 30' at 4°C. Pellets were resuspended in sample buffer and supernatants were resuspended in sample buffer following TCA precipitation.

Live Cell imaging: For imaging experiments, the cells were pre-incubated in a serum-free extracellular medium (ECM, 121 mM NaCl, 5 mM $NaHCO_3$, 10 mM Na-HEPES, 4.7 mM KCl, 1.2 mM KH_2PO4, 1.2 mM $MgSO_4$, 2 mM $CaCl_2$, 10 mM glucose, pH7.4) containing 2% BSA. For permeabilized cell experiments, the transfected cells were washed with a Ca^{2+}-free ECM containing 100 μM EGTA/TRIS and transferred to the imaging chamber in 1 ml intracellular medium (ICM, composed of 120 mM KCl, 10 mM NaCl, 1 mM KH_2PO_4, 20 mM Tris-HEPES at pH 7.2, 2 mM MgATP. Plasma membrane permeabilization was carried out using saponin 40 μg/ml. After 5 min permeabilization (35°C), the cells were washed into fresh ICM supplemented with succinate/TRIS 2 mM, 10 μM EGTA/TRIS and rhod2/FA 0.5 μM.

Fluorescence wide field imaging of $[Ca^{2+}]_c$, $[Ca^{2+}]_m$, pH_m and $\Delta\Psi_m$ was carried out using a ProEM1024 EM-CCD (Princeton Instruments), fitted to Leica DMI 6000B inverted epifluorescence microscopes. When both $[Ca^{2+}]_c$ and $[Ca^{2+}]_m$ were recorded, with fura2 and ipcam, 340/30nm, 380/20nm, and 490/20nm excitation filters were used with beam splitter 500 nm and emission filter 540/50nm and an image triplet was obtained in every 2s. The fura2 ratios were calibrated in terms of nM $[Ca^{2+}]_c$, whereas the ipcam fluorescence at each time point was normalized to the initial fluorescence (F_0/F). When $[Ca^{2+}]_m$ was measured with rpcam or H_2O_2 with HyPer or pH_m with SypHer, 490/20 nm and 415/20 nm excitation filters and a 500 nm long-pass beam splitter were used and an image pair was obtained in every 2 s. $[Ca^{2+}]_m$ is shown as F_0/F of the fluorescence recorded at 415 nm excitation, which is insensitive to pH changes. When both $[Ca^{2+}]_c$ and $\Delta\Psi_m$ were measured with fura2 or furaFF and TMRE, 2 different filter sets (for TMRE: ex:580/20 nm, bs595 nm, em: 630/60 nm) were alternated by a motorized turret.

Measurements of ^{45}Ca uptake in suspensions of permeabilized cells: Suspensions of cells ($2x10^6$/ml) were permeabilized in ICM containing 2 μM Tg to inhibit ER Ca^{2+} uptake and 10 μM EGTA to maintain $[Ca^{2+}] \leq 20$nM and 2 mM succinate, to energize mitochondria and saponin 40 μg/ml at 37°C. Subsequently, suspensions were mixed with 4 μCi/ml ^{45}Ca ($[Ca^{2+}]$ approx 30 μM) in the absence or presence of RuRed (3 μM). At 60, 150, 300 and 450 s time points 100 μl aliquots were diluted in 5 ml ice cold washing buffer (KCl 140mM, Hepes/TRIS 10 mM, EGTA/TRIS 0.5 mM, pH7.2) and filtered through 0.3 μm nitrocellulose filters (Millipore). Filters were rinsed once with washing buffer. ^{45}Ca in the cells remaining on the filters were quantified by liquid scintillation counting.

Measurement of cellular oxygen consumption: JO_2 was measured using an XF24 Extracellular Flux analyzer (Seahorse Biosciences), at 37°C. Cells were seeded at 20-30,000/well onto 24-well plates the day before experiments. Measurements were made in Ca^{2+} and glucose-free ECM containing, 5 mM lactate and 0.5 mM pyruvate, and 50 μM EGTA. Tg (2 μM) was injected 12 min prior to $CaCl_2$ injection. For each JO_2 measurement, JO_2 was measured over 2 min, followed by 2 min mix and 2 min delay intervals.

Cell death analysis. Cells, grown in 6-well plates, were serum-starved for 1 hr in ECM. Then either 100 μM H_2O_2 or solvent was added for 10 min followed by 2 μM Tg for 1 hr. At the end of the incubation, cell viability and number were determined by Trypan blue exclusion and cell counting on a hemocytometer, respectively.

Modeling of Ca^{2+} release after uncoupling: For analysis of post-FCCP Ca^{2+} release data, the period of 3–33 seconds post-FCCP addition from 7 runs each of control and MICU1-KD cells was fitted by both exponential and logistic curves ($R^2 \geq .994$ for all fits). The resulting curves were differentiated to obtain the instantaneous rates of Ca^{2+} release after depolarization, which were replotted as a function of the $[Ca^{2+}]_c$ at each point. The histograms (Fig5B) were generated from the exponential fit data described above, by binning the resultant Ca^{2+} uptake rates by 0.5μM $[Ca^{2+}]_c$ concentrations. The data from the logistic regressions were compiled and fitted by exponential rise to maximum curves shown in Fig3E (R^2 = .991 and .639 for control and KD respectively). High-pass 'Butterworth filter' modeling referred in the text was according to the transfer function of the form (a/(1+(x0/x)^b))^0.5. EF-hand mutant and RESCUE data are from 4 runs each analyzed by the same methods.

Supplemental References

Baughman, J.M., Perocchi, F., Girgis, H.S., Plovanich, M., Belcher-Timme, C.A., Sancak, Y., Bao, X.R., Strittmatter, L., Goldberger, O., Bogorad, R.L*., et al.* (2011). Integrative genomics identifies MCU as an essential component of the mitochondrial calcium uniporter. Nature.

Csordas, G., Varnai, P., Golenar, T., Roy, S., Purkins, G., Schneider, T.G., Balla, T., and Hajnoczky, G. (2010). Imaging interorganelle contacts and local calcium dynamics at the ER-mitochondrial interface. Molecular cell *39*, 121-132.

Giacomello, M., Drago, I., Bortolozzi, M., Scorzeto, M., Gianelle, A., Pizzo, P., and Pozzan, T. (2010). Ca2+ hot spots on the mitochondrial surface are generated by Ca2+ mobilization from stores, but not by activation of store-operated Ca2+ channels. Molecular cell *38*, 280-290.

Nagai, T., Sawano, A., Park, E.S., and Miyawaki, A. (2001). Circularly permuted green fluorescent proteins engineered to sense Ca2+. Proceedings of the National Academy of Sciences of the United States of America *98*, 3197-3202.

Perocchi, F., Gohil, V.M., Girgis, H.S., Bao, X.R., McCombs, J.E., Palmer, A.E., and Mootha, V.K. (2010). MICU1 encodes a mitochondrial EF hand protein required for Ca(2+) uptake. Nature *467*, 291-296.

Poburko, D., Santo-Domingo, J., and Demaurex, N. (2011). Dynamic regulation of the mitochondrial proton gradient during cytosolic calcium elevations. The Journal of biological chemistry *286*, 11672-11684.

Roy, S.S., Madesh, M., Davies, E., Antonsson, B., Danial, N., and Hajnoczky, G. (2009). Bad targets the permeability transition pore independent of Bax or Bak to switch between Ca2+-dependent cell survival and death. Molecular cell *33*, 377-388.

Ryan, M.T., Voos, W., and Pfanner, N. (2001). Assaying protein import into mitochondria. Methods in cell biology *65*, 189-215.

Sato, T., and Mihara, K. (2010). Mammalian Oxa1 protein is useful for assessment of submitochondrial protein localization and mitochondrial membrane integrity. Analytical biochemistry *397*, 250-252.

Schmittgen, T.D., and Livak, K.J. (2008). Analyzing real-time PCR data by the comparative C(T) method. Nat Protoc *3*, 1101-1108.